Structure properties of medium and heavy exotic nuclei

M. K. Gaidarov

Institute for Nuclear Research and Nuclear Energy, Bulgarian Academy of Sciences, Sofia 1784, Bulgaria

E-mail: gaidarov@inrne.bas.bg

Abstract. Investigations of important characteristics of the structure of nuclei near drip-lines in coordinate and momentum space have been performed. The charge form factors, charge and matter densities and the corresponding rms radii for even-even isotopes of Ni, Kr, and Sn are calculated in the framework of deformed self-consistent mean field Skyrme DDHF+BCS method. The resulting charge radii and neutron skin thicknesses of these nuclei are compared with available experimental data, as well as with other theoretical predictions. The formation of a neutron skin is analyzed in terms of various definitions. Its correlation with the nuclear symmetry energy is studied within the coherent density fluctuation model using the symmetry energy as a function of density within the Brueckner energy-density functional. The nucleon momentum distributions for the same isotopic chains of neutron-rich nuclei are studied in the framework of the same mean-field method, as well as of theoretical correlation methods based on light-front dynamics and local density approximation. The isotopic sensitivities of the calculated neutron and proton momentum distributions are investigated together with the effects of nucleon correlations and deformation of nuclei.

1. Introduction

The detailed study of the properties of unstable nuclei far from the stability line has been one of the main goals of nuclear physics in the last years. Recently, the development of radioactive ion beam facilities in GSI (Germany) and in RIKEN (Japan) has opened a new field for such studies, making possible the production of a variety of exotic nuclei that may have large neutron or proton excess.

In the present study, the properties of even-even Ni, Kr, and Sn isotopes are described using the deformed self-consistent density-dependent Hartree-Fock (DDHF) mean-field method with Skyrme-type effective interactions (DDHF+BCS method). These are the charge form factors, the neutron and proton skins in neutron-rich and neutron-deficient isotopes, respectively, the nuclear symmetry energy and the nucleon momentum distributions. We choose some medium and heavy Ni, Kr, and Sn isotopes because many of these sets, which lie in the nuclear chart between the proton and neutron drip lines can be formed as radioactive ions to perform scattering experiments. The main goal of this study is to perform theoretical analyses of exotic nuclear structure properties which can be a step in a future comparison between the predicted characteristics and the results of possible experiments using colliding electron-exotic nuclei storage rings thus showing the effect of the neutron excess in these nuclei.

Published under licence by IOP Publishing Ltd

2. Densities and charge form factors

The most realistic description of elastic electron-scattering cross sections can be achieved by solving the Dirac equation and performing an exact phase-shift analysis [1]. This method has been chosen, e.g. in Ref. [2] (see also Ref. [3] for the ELISe experiment). Using it, the modulus of the charge form factor can be determined from the differential cross section. Its sensitivity to changes in the charge distribution is demonstrated in Fig. 1, where Ni isotopes are shown as example. The proton densities presented in Fig. 1 were obtained from self-consistent DDHF+BCS mean-field calculations with effective nucleon-nucleon (NN) interactions in a large harmonic-oscillator basis [4] by using a density-dependent Skyrme parametrization. In the same figure, the squared moduli of charge form factors, which are obtained from solving the Dirac equation numerically, are presented. Following this prescription, electron scattering is computed in the presence of a Coulomb potential induced by the charge distribution of a given nucleus. The intrinsic charge distribution of the neutron is included into these calculations.

The nuclear charge form factor $F_{ch}(q)$ has been calculated as

$$F_{ch}(q) = \left[F_{point,p}(q)G_{Ep}(q) + \frac{N}{Z}F_{point,n}(q)G_{En}(q)\right] F_{c.m.}(q), \tag{1}$$

where $F_{point,p}(q)$ and $F_{point,n}(q)$ denote the form factors related to the point-like proton and neutron densities $\rho_{point,p}(\mathbf{r})$ and $\rho_{point,n}(\mathbf{r})$, respectively [2]. These densities correspond to wave functions in which the positions $\mathbf{r}$ of the nucleons are defined with respect to the centre of the potential in the laboratory system. In order to let $F_{ch}(q)$ correspond to the density distributions in the center-of-mass coordinate system, a factor $F_{c.m.}(q)$ is introduced in a commonly used way [5]:

$$F_{c.m.}(q) = e^{(qR)^2/6A}, \tag{2}$$

where R stands for the root-mean-square (rms) radius of the nucleus. Eq. (1) with a c.m. correction of form (2) was used to compute the modulus squared of the form factor that can be extracted also from experimental data. In Eq. (1) $G_{Ep}(q)$ and $G_{En}(q)$ denote Sachs proton and neutron electric form factors, respectively, and are taken from one of the most recent

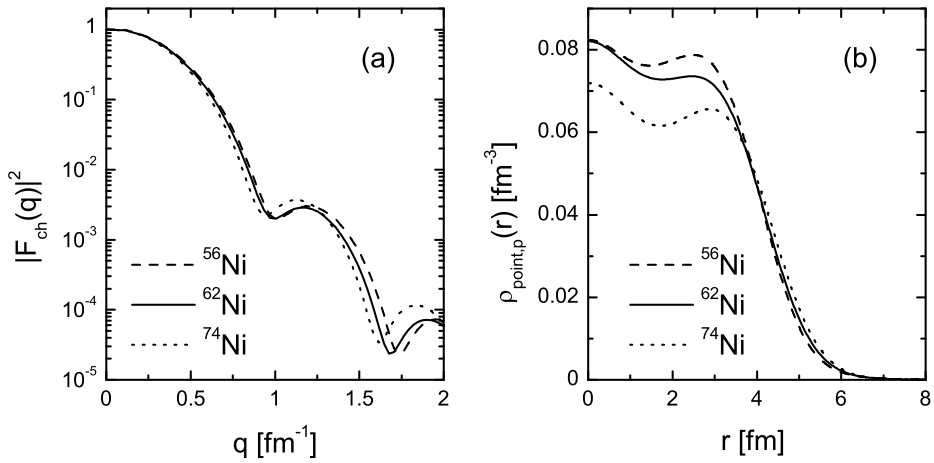

Figure 1. Modulus squared of charge form factors (panel (a)) calculated by solving the Dirac equation with DDHF+BCS proton densities (panel (b)) for the unstable double-magic ^{56}Ni, stable ^{62}Ni and unstable ^{74}Ni isotopes [2].

phenomenological parametrizations [6]. In general, it has been found that with increasing number of neutrons in a given isotopic chain the minima of the curves of the charge form factor are shifted towards smaller values of the momentum transfer [2]. This is due mainly to the enhancement of the proton densities in the peripheral region and to a minor extent to the contribution from the charge distribution of the neutrons themselves. By accounting for the Coulomb distortion of the electron waves, a filling of the Born zeros is observed when the distorted-wave method is used (in contrast to plane-wave Born approximation).

3. Neutron skins from Skyrme Hartree-Fock calculations. Nuclear symmetry energy

The thickness of a neutron skin in nuclei may be defined in different ways. One of these possibilities is to determine it as the difference between the rms radius of neutrons and that of protons. In Fig. 2 we plot this difference $\Delta r_{np} = r_n - r_p$, where on the left panel we show our results with the SLy4 force [7] for Sn isotopes and compare them with the predictions from relativistic mean-field (RMF) model [8] and to experimental data taken from (p, p) scattering [9, 10], antiprotonic atoms [11], giant dipole resonance method [12], and spin dipole resonance method [13, 14]. As can be seen in Fig. 2 the experimental data are located between the predictions of both theoretical approaches and in general, there is agreement with the experiment within the error bars. On the right panels we see the predictions for Δr_{np} in the cases of Ni and Kr isotopes, where there are no data. The RMF results for the difference Δr_{np} systematically overestimate the Skyrme HF results, as it can be seen from Fig. 2. The reason for this is related to the difference in the nuclear symmetry energy and, consequently, to the different neutron equation of state (EOS) which has been extensively studied in recent years. It was shown that there exists a linear correlation between the derivative of the neutron EOS (or the pressure of neutron matter) and the neutron skin thickness in heavy nuclei in both Skyrme HF [15, 16] and RMF [16, 17] models.

Therefore, in Ref. [18] we investigate the relation between the neutron skin thickness and some nuclear matter properties in finite nuclei, such as the symmetry energy at the saturation point s, symmetry pressure p_0 (proportional to the slope of the bulk symmetry energy), and asymmetric compressibility ΔK, considering nuclei in given isotopic chains and within a certain theoretical approach. As the main emphasis is to inspect the correlation of the neutron skin thickness ΔR of nuclei in a given isotopic chain with the s, p_0 and ΔK parameters extracted from the density dependence of the symmetry energy around the saturation density, we show in Fig. 3 the results for Ni isotopes. The symmetry energy, the pressure and the asymmetric compressibility are calculated within the coherent density fluctuation model (CDFM) (e.g., Ref. [19]) by using the weight functions calculated from the DDHF+BCS densities (for more details, see Ref. [18]). In addition, it is important to note that we obtain the symmetry energy in finite nuclei including both bulk and surface contributions on the base of the Brueckner EOS. It is seen from Fig. 3(a) that there exists an approximate linear correlation between ΔR and s for the even-even Ni isotopes with $A = 74 - 84$. We observe a smooth growth of the symmetry energy till the double-magic nucleus ^{78}Ni ($N = 50$) and then a linear decrease of s while the neutron skin thickness of the isotopes increases. This behavior is valid for all Skyrme parametrizations used in the calculations, in particular, the average slope of ΔR for various forces is almost the same. We also find a similar approximate linear correlation for Ni isotopes between ΔR and p_0 [Fig. 3(b)] and a less strong correlation between ΔR and ΔK [Fig. 3(c)]. As in the symmetry energy case, the behavior of the curves drawn in these plots shows the same tendency, namely the inflexion point transition at the double-magic ^{78}Ni nucleus.

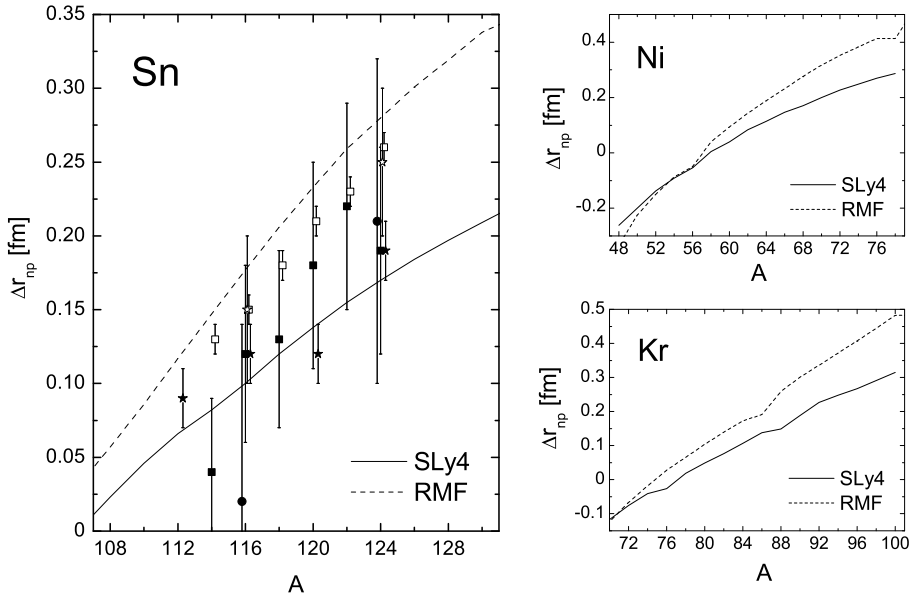

Figure 2. Difference between neutron and proton rms radii Δr_{np} of Sn, Ni, and Kr isotopes calculated with SLy4 force. The RMF calculation results are from Ref. [8]. The experimental data for Sn isotopes measured in (p, p) reaction (open stars) [9, 10], antiproton atoms (full stars) [11], giant dipole resonance method (full circles) [12] and spin dipole resonance method (full and open squares) [13, 14] are also shown.

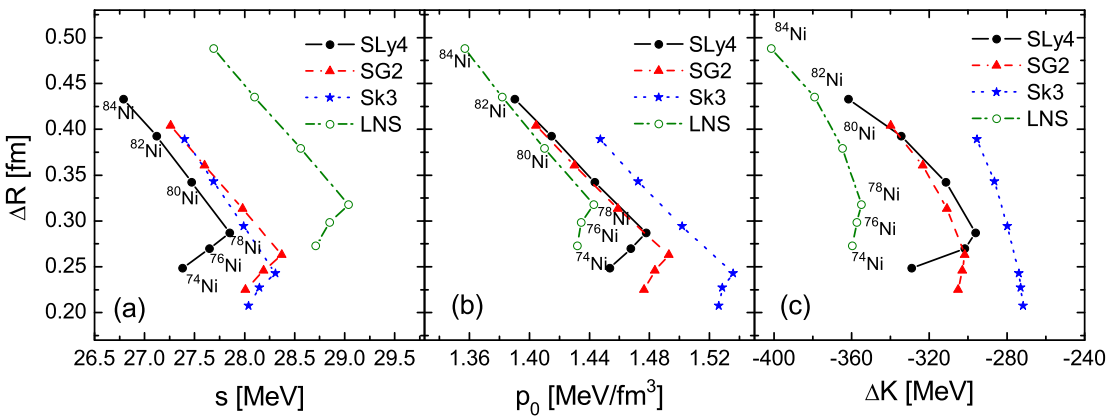

Figure 3. HF+BCS neutron skin thicknesses ΔR for Ni isotopes as a function of the symmetry energy s (a), pressure p_0 (b), and asymmetric compressibility ΔK (c) calculated with SLy4, SG2, Sk3, and LNS forces.

4. Momentum distributions

Another important characteristic of the nuclear ground state is the nucleon momentum distribution (NMD) $n(k)$. The scaling analyses of inclusive electron scattering from a large variety of nuclei showed the evidence for the existence of high-momentum components of NMD at momenta $k > 2$ fm^{-1}. It has been shown that it is due to the presence of NN correlations in nuclei (for a review, see e.g. [19]). It is of importance to study the NMD not only in stable, but also in exotic nuclei [20]. As an example, the neutron and proton momentum distributions

of ^{64}Ni, ^{84}Kr, and ^{120}Sn nuclei calculated within the DDHF+BCS method and two correlation approaches, namely the one from [21] using the light-front dynamics (LFD) method and the other [22] based on the local density approximation (LDA), are presented in Fig. 4. As can be seen, for all nuclei the inclusion of NN correlations strongly affects the high-momentum region of NMD. At $k > 1.5$ fm^{-1} both LFD and LDA momentum distributions start to deviate from the DDHF+BCS case. They behave rather similar in the interval $1.5 < k < 3$ fm^{-1}. At $k > 3$ fm^{-1} the LFD method predicts systematically higher momentum components compared to LDA momentum distributions. This observation can be explained by the different extent to which NN correlations are taken into account in both approaches. Our results for the NMD's in the LFD method for large values of k ($k > 2$ fm^{-1}) are similar to those obtained within the Jastrow correlation method and, thus, the high-momentum tails of $n(k)$ are caused by the short-range NN correlations. The LDA approach through the nuclear matter dynamic effects and using the local Fermi momentum $k_F^{Z(N)}(r)$ calculated self-consistently by means of the HF density produces less pronounced high-momentum tail, but still the results are very close to those obtained in the LFD method. As was expected, at $k > 1.5$ fm^{-1} the DDHF+HF momentum distributions fall off rapidly by several orders of magnitude in contrast to the correlated NMD's. In addition, we observe that: i) the results shown above are similar for all nuclei in a given isotopic chain and going from Ni to Sn isotopes, as well; ii) the behavior of $n(k)$ is similar for protons and neutrons; iii) at high k the proton and neutron NMD's obtained within the LFD method cannot be distinguished from each other because the high-momentum tails in this approach are determined by the high-momentum component of the nucleons in the deuteron [21]; iv) concerning the NMD's calculated in the LDA approach, some difference between $n(k)$ for protons and neutrons can be observed due to $Z(N)$-dependence of the local Fermi momentum k_F.

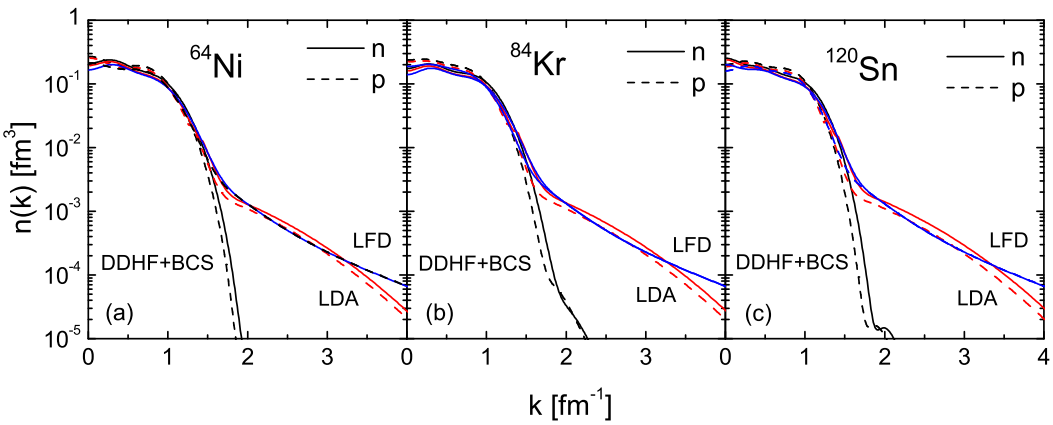

Figure 4. Neutron (solid line) and proton (dashed line) momentum distributions obtained within the DDHF+BCS, LFD, and LDA methods for ^{64}Ni (a), ^{84}Kr (b), and ^{120}Sn (c) nuclei.

5. Conclusions

The results of the present work can be summarized as follows:

i) There is a decrease of the proton densities in the nuclear interior and an increase of its tail at large r with increasing neutron number. Consequently, the common feature of the charge form factors is the shift of the form factor curves and their minima to smaller values of q with the increase of the neutron number in a given isotopic chain. The theoretical predictions for the charge form factors of exotic nuclei are a challenge for their measurements in the future

experiments in GSI and RIKEN and thus, for obtaining detailed information on the charge distributions of such nuclei.

ii) For a given isotopic chain, the increase of the skin with N exhibits a rather constant slope, which is different depending on the definition of nuclear skin. A pronounced neutron skin can be attributed to isotopes with $A > 132$ for Sn, $A > 74$ for Ni, and $A > 96$ for Kr. While the radial extensions of the densities in deformed nuclei (prolate and oblate) change with the direction, the neutron skin thickness remains practically constant along the different directions.

iii) We have demonstrated the capability of CDFM to be applied as an alternative way to make a transition from the properties of nuclear matter to the properties of finite nuclei investigating the nuclear symmetry energy s, the neutron pressure p_0 and the asymmetric compressibility ΔK in finite nuclei.

iv) A possible practical way to make predictions for the momentum distributions of exotic nuclei far from the stability line is proposed that provides a systematic description of $n(k)$ in medium-weight and heavy nuclei.

Acknowledgments

This study is performed together with Professor A. N. Antonov, Dr. D. N. Kadrev and Dr. M. V. Ivanov from the Institute for Nuclear Research and Nuclear Energy of the Bulgarian Academy of Sciences, Professor V. K. Lukyanov and Professor E. V. Zemlyanaya from the Joint Institute for Nuclear Research, Dubna, Russia, Dr. G. Z. Krumova from the University of Ruse, Bulgaria, Professor P. Sarriguren from the Instituto de Estructura de la Materia, CSIC, Madrid, Spain, and Professor E. Moya de Guerra and Professor J. M. Udias from the Complutense University, Madrid, Spain, to whom I would like to express my warmest thanks. All Bulgarian authors are grateful for the support of the Bulgarian Science Fund under Contract No. 02–285.

References

[1] Yennie D R, Ravenhall D G and Wilson R N 1954 *Phys. Rev.* **95** 500 (and references therein)
[2] Antonov A N, Kadrev D N, Gaidarov M K, Moya de Guerra E, Sarriguren P, Udias J M, Lukyanov V K, Zemlyanaya E V and Krumova G Z 2005 *Phys. Rev.* C **72** 044307
[3] Antonov A N *et al.* 2011 *Nucl. Instr. and Meth.* A **637** 60
[4] Sarriguren P, Moya de Guerra E and Escuderos A 1999 *Nucl. Phys.* A **658** 13; 2001 *Phys. Rev.* C **64** 064306
[5] Burov V V and Lukyanov V K 1977 *JINR Preprint, Dubna* **R4-11098**; Burov V V, Kadrev D N, Lukyanov V K and Pol' Yu S 1998 *Phys. At. Nucl.* **61** 525
[6] Friedrich J and Walcher Th 2003 *Eur. Phys. J.* A **17** 607
[7] Sarriguren P, Gaidarov M K, Moya de Guerra E and Antonov A N 2007 *Phys. Rev.* C **76** 044322
[8] Lalazissis G A, Raman S and Ring P 1999 *At. Data Nucl. Data Tables* **71** 1
[9] Ray L *et al.* 1979 *Phys. Rev.* C **19** 1855
[10] Hoffmann G W *et al.* 1981 *Phys. Rev. Lett.* **47** 1436
[11] Trzcinska A *et al.* 2001 *Phys. Rev. Lett.* **87** 082501
[12] Krasznahorkay A *et al.* 1994 *Nucl. Phys.* A **567** 521
[13] Krasznahorkay A *et al.* 1999 *Phys. Rev. Lett.* **82** 3216
[14] Krasznahorkay A *et al.* 2004 *Nucl. Phys.* A **731** 224
[15] Brown B A 2000 *Phys. Rev. Lett.* **85** 5296
[16] Furnstahl R J 2002 *Nucl. Phys.* A **706** 85
[17] Typel S. and Brown B A 2001 *Phys. Rev.* C **64** 027302
[18] Gaidarov M K, Antonov A N, Sarriguren P and Moya de Guerra E 2011 *Phys. Rev.* C **84** 034316
[19] Antonov A N, Hodgson P E and Petkov I Zh 1988 *Nucleon Momentum and Density Distributions in Nuclei* (Clarendon Press, Oxford); 1993 *Nucleon Correlations in Nuclei* (Springer-Verlag, Berlin-Heidelberg-New York)
[20] Gaidarov M K, Krumova G Z, Sarriguren P, Antonov A N, Ivanov M V and Moya de Guerra E 2009 *Phys. Rev.* C **80** 054305
[21] Antonov A N, Gaidarov M K, Ivanov M V, Kadrev D N, Krumova G Z, Hodgson P E and von Geramb H V 2002 *Phys. Rev.* C **65** 024306
[22] Stringari S, Traini M and Bohigas O 1990 *Nucl. Phys.* A **516** 33